

Molecular dynamics study of damage accumulation in GaN during ion beam irradiation

J. Nord, K. Nordlund, and J. Keinonen

Accelerator Laboratory, P.O. Box 43, University of Helsinki, FIN-00014, Finland

(Received 28 May 2003; revised manuscript received 6 August 2003; published 7 November 2003)

We have used molecular dynamics methods to study the accumulation of damage during ion beam irradiation of GaN. First we analyzed individual recoils between 200 eV and 10 keV. We found that the spatial average of the threshold displacement energy was high and much less damage was produced in GaN than in Si, Ge, or GaAs cascades. Most of the damage was in isolated point defects or small clusters, which enhances the damage recombination probability. Ion beam amorphization was simulated by starting successive 400-eV or 5-keV recoils in an initially perfect crystal. The development of volume, energy, and ring statistics, as well as segregation of compounds, was followed through the process. The simulations show that the amorphization begins with single defects and formation of long weak Ga-Ga bonds in the distorted lattice. We also observe that nitrogen gas is produced during prolonged irradiation, in agreement with experimental observations. We recognize two reasons for the high amorphization dose of GaN, the high threshold displacement energy and different varieties of in-cascade recombination.

DOI: 10.1103/PhysRevB.68.184104

PACS number(s): 64.70.Kb, 61.43.Dq, 61.72.Cc, 61.82.Fk

I. INTRODUCTION

GaN is an important compound semiconductor material especially for optoelectronic applications. It has a large direct band gap and is hard and chemically inert. For many applications, ion beam implantation of doping atoms is a useful tool for modifying the material properties. For a successful application of the implantation, it is important to understand the production of damage in GaN during irradiation.

Experimental studies on ion beam amorphization of GaN have revealed the complexity of the process.¹⁻¹⁰ For heavy ions and low temperatures (less than 80 K), two amorphous peaks have been observed;^{6,7,9,10} one at the surface and another in the bulk. At higher temperatures saturation of the damage peak occurs in the bulk^{6-8,10} and amorphization proceeds from the surface. In the case of silicon irradiation, the damage saturates in the bulk for both 77 K and 300 K temperatures, and the amorphous area grows from the surface.⁷ For lighter C and O ions, the damage level in the bulk does not saturate at 77 K or 300 K,^{6,7,10} but two intermediate saturation levels have been found in a recent study⁹ at 15 K, where thermal annealing can be ruled out. Even further, the level at which the damage saturates for 300 K implantation of heavy ions depends on the ion species.⁷ Dynamic annealing¹¹ and chemical effects for light ions have been proposed to explain some of these issues,^{1,2,7,8,10} but much remains poorly understood.

The reported amorphization doses depend strongly on the implantation conditions: the displacements per atom vary from about 5 dpa (damage level at the border of the amorphous area for 180 keV Ar at 77 K temperature⁴) and 10 dpa [measured at the damage peak for surface amorphization at 180 K for Au (Ref. 8)] to 60 dpa [in bulk at 300 K (Ref. 8) for Au]. The amorphization doses are 1-3 orders of magnitude higher than the dose for Si or GaAs.^{1,3,4,9} The high variation in the results and complex interaction between implantation parameters and observed behavior complicates the interpretation of the experimental findings.

Molecular dynamics computer simulations are a useful

tool for studying irradiation induced damage processes. Until recently such simulations were restricted by the lack of an interatomic potential model, which could describe far-from-equilibrium processing of GaN.

The paper is organized as follows. The simulation methods are explained in Sec. II. In Sec. III, we first examine the threshold displacement energy (Sec. III A) and the damage in individual cascades (Sec. III B). After that we examine the amorphization process (Sec. III C) and the structure of the amorphous GaN (Sec. III D). The results are discussed in Sec. IV and the paper is concluded in Sec. V.

II. METHOD

To study irradiation effects in GaN, we used molecular dynamics methods and an analytical potential model. Damage production was studied both in individual cascades and during prolonged irradiation.

GaN simulation cells were created using the wurtzite (WZ) crystal structure with an orthogonal unit cell corresponding to two conventional hexagonal unit cells. The damage production in individual cascades was studied by starting a recoil in the middle of the simulation cell. Energies varying from 200 eV to 10 keV were used, and the number of atoms in the simulation cell was between 7000 and 1 800 000. Since we are primarily interested in bulk damage, periodic boundary conditions were used in three dimensions. To remove the excess heat energy from the cell, Berendsen temperature control¹³ was applied near the borders of the simulation cell. The simulation method is discussed in more detail in Ref. 14.

We simulated the amorphization process during prolonged irradiation by starting successive 400-eV or 5-keV recoils in initially perfect cells with 14 000 or 59 000 atoms. A two-phase iteration scheme was used to model the continuous irradiation. In the first phase, a recoil is started from the center of the cell, and the process is simulated as an individual recoil event. After the cell has cooled down, the sec-

ond phase is initiated. In this relaxation phase, the system is effectively cooled down to 0 K as the Berendsen pressure control¹³ is applied to the whole cell and pressure is relaxed to zero. After the relaxation, all atoms in the cell are shifted randomly a distance $(u_1 S_x, u_2 S_y, u_3 S_z)$, where u_1, u_2 , and u_3 are random numbers in the range 0–1, and (S_x, S_y, S_z) is the cell size. After this the periodic boundary conditions are used to bring the atoms outside the cell back on the other side. In this way the starting point of the next recoil is random in continuous periodic space. Then the iteration is continued with a new recoil.

Using this approach, homogeneous periodic amorphous cells can be generated. The method, which has been previously successfully applied in Si, Ge, and GaAs, is described in more detail elsewhere.¹⁵

The forces between the atoms were described by a classical many-body potential model for GaN.¹² Since we also study high-dose irradiation, it is important to note that the model describes well pure Ga and N phases also. The model does not include long-range Coulombic interactions, but many properties (such as melting, point defect properties, and elastic moduli), important for the modeling of far-from-equilibrium effects, are well described by this potential model. We have compared the primary damage of GaN simulated with ionic and nonionic potential models.¹⁶ Our initial results show that the damage level in the ionic model is within a factor of ~ 2 compared to the nonionic model. Such a difference might be related to the potential fitting as well, and is not large enough to explain the order-of-magnitude difference in the damage level between GaAs and GaN. The ionicity may affect the defect migration and recombination properties, but these long time scale effects are not readily accessible with molecular dynamics.

During the amorphization process, the development of the cell volume, average potential energy, ring statistics, and the segregation of compounds was followed. The defects were recognized by using the Voronoy-polyhedron approach. The positions of the atoms after the recoil event were assigned to belong to some Voronoy polyhedron of the initial lattice configuration. An empty polyhedron was considered a vacancy. If a multiply filled polyhedron contained atoms of the same type as it initially contained, all atoms except the initial one were counted as interstitials. Otherwise one of the atoms was counted as an antisite and the others as interstitials. Also, atoms on a singly filled polyhedron of a wrong type were considered antisites.

III. RESULTS

A. Threshold displacement energy

We studied the threshold displacement energy for Ga and N recoils in wurtzite GaN by starting recoils from perfect lattice sites in 1000 random directions. The threshold displacement values were searched by a binary search algorithm for each direction as follows. We first set upper (200 eV) and lower (0 eV) limits for the threshold displacement energy. A recoil energy with the average value of upper and lower limits was then selected for testing. After the recoil event was simulated, the total energy of the cell was calculated. If the

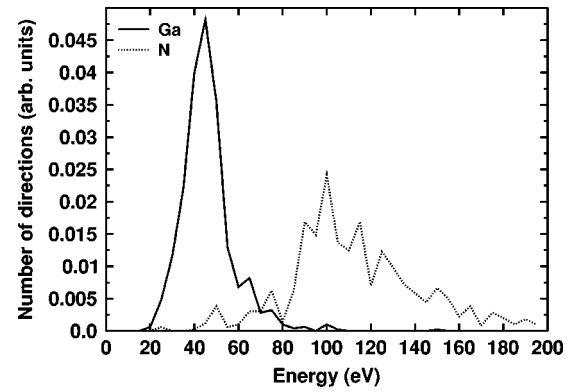


FIG. 1. Area density of different threshold displacement energies for Ga and N recoils in WZ GaN.

total energy was higher than 1 eV over the value of a perfect crystal, a displacement was assumed. This cutoff value was chosen after visually confirming a displacement in several recoil events. If a displacement occurred, the upper limit was set to the current recoil energy. Otherwise the lower limit was set to the recoil energy. This process was iterated until the difference between upper and lower limits was less than 1 eV.

The distributions of different energies for both atom types are shown in Fig. 1. Although the lowest values for the threshold displacement energy are small (18 ± 1 eV for Ga and 22 ± 1 eV for N), the average values are considerably high (45 ± 1 eV for Ga and 109 ± 2 eV for N). This high average threshold displacement partly explains the small amount of damage produced in individual cascades and the high amorphization dose. The lowest threshold displacement energy value for Ga is in excellent agreement with the direct experimental value of 19 ± 2 (Ref. 17).

The smallest value for the threshold displacement energy for nitrogen is in a direction about 10° angle off the c axis, away from the Ga bond in the (0001) direction. For gallium, the minimum is obtained toward the second-nearest Ga neighbor on the negative side of the c axis.

B. Primary damage states in individual cascades

The primary damage states produced in individual cascades were studied for recoil energies between 200 eV and 10 keV. The number of interstitials, vacancies, and antisites is shown in Table I. A comparison with GaAs in Fig. 2 shows that much less damage is produced in GaN than in GaAs. About a factor of 5 for the difference in the amorphization doses is explained by the low damage production in individual cascades, which is related to a high threshold displacement energy as explained in Sec. III A. Figure 2 also shows that there is a dip in the damage production after a recoil energy of 1 keV. The effect is akin to metals, where the molten areas in a heat spike can recrystallize efficiently and produce almost intact lattice.¹⁸ To examine the local heating effect, we calculated the average temperature of the atoms closer than 13 \AA to the energy-weighted cascade center. The results for representative 1-, 2-, and 5-keV recoil events are presented in Fig. 3. The region between 200 fs and about 5

TABLE I. Average production of point defects in 200 eV–10 keV cascades in GaN for N and Ga recoils.

E (eV)	V_N	V_{Ga}	I_N	I_{Ga}	N_{Ga}	Ga_N
N recoils						
200	1.0 ± 0.1	0.12 ± 0.05	0.80 ± 0.09	0.32 ± 0.07	0.22 ± 0.06	0.02 ± 0.02
400	1.3 ± 0.2	1.4 ± 0.2	1.3 ± 0.2	1.4 ± 0.1	0.43 ± 0.09	0.33 ± 0.09
1000	3.3 ± 0.3	2.1 ± 0.4	2.7 ± 0.3	2.8 ± 0.3	1.3 ± 0.2	0.71 ± 0.20
2000	3.9 ± 0.9	5.3 ± 0.9	3.1 ± 0.6	6.0 ± 0.7	1.5 ± 0.6	0.75 ± 0.25
5000	11.2 ± 1.0	11.3 ± 1.0	9.9 ± 0.8	12.6 ± 1.1	4.2 ± 0.6	2.9 ± 0.4
10000	29.5 ± 2.7	21.4 ± 0.9	24.9 ± 1.9	26.0 ± 1.1	12.4 ± 1.2	7.8 ± 0.9
Ga recoils						
200	0.32 ± 0.05	1.3 ± 0.1	0.40 ± 0.06	1.2 ± 0.1	0.02 ± 0.01	0.12 ± 0.03
400	1.2 ± 0.2	1.8 ± 0.1	1.2 ± 0.1	1.8 ± 0.1	0.30 ± 0.07	0.26 ± 0.06
1000	4.0 ± 0.4	3.1 ± 0.3	3.6 ± 0.4	3.5 ± 0.3	1.3 ± 0.2	0.80 ± 0.21
2000	6.1 ± 0.5	4.8 ± 0.5	4.9 ± 0.4	6.0 ± 0.6	1.2 ± 0.2	2.4 ± 0.4
5000	13.1 ± 1.0	11.3 ± 0.6	11.3 ± 0.4	13.1 ± 1.0	4.6 ± 0.7	2.8 ± 0.5
10000	24.6 ± 2.2	22.1 ± 1.4	21.8 ± 2.2	25.0 ± 1.4	8.8 ± 1.5	5.9 ± 1.4

ps, where the temperature in the volume is almost constant, indicates the presence of a heat spike. This in-cascade recombination is another reason for the high amorphization dose, but the effect is smaller (only about a factor of 1–2) than that caused by the high effective threshold displacement energy (about a factor of 5).

Damage clusters are harder to anneal than individual defects. Therefore we performed a cluster analysis for the damage in individual cascades. We considered interstitials and vacancies closer than 4.5 Å to each other to belong to the same cluster. Table II shows the percentage of interstitials and vacancies in clusters larger than six defects for different recoil atom types and energies. Antisite defects are more clustered than other defects. About 30–50 % of the antisites are in clusters for nitrogen recoils and about half for gallium recoils. The majority of the damage is isolated at all the studied energies. The damage is especially strongly scattered for 2-keV nitrogen recoils, where less than 5% of the damage

is in clusters. The small amount of clusters in this case is explained by the small weight of N. Since most of the damage is in point defects or small clusters (smaller than six defects), it is likely that a large amount of damage can be annealed after small irradiation doses. The large volume of cascades and low defect concentration mean that multiple passes of ions are needed to amorphize the material in a given spatial region.

C. Amorphization process

Experiments have shown that GaN is much harder to amorphize than many other common semiconductor materials, such as Si, Ge, or GaAs. It has been estimated that the doses needed to amorphize GaN and GaAs may differ as much as 1–3 orders of magnitude.^{1,4} The high amorphization dose can be partly explained by the properties of individual cascades discussed elsewhere in this paper. Previously, dynamic annealing¹¹ had been proposed to explain the experi-

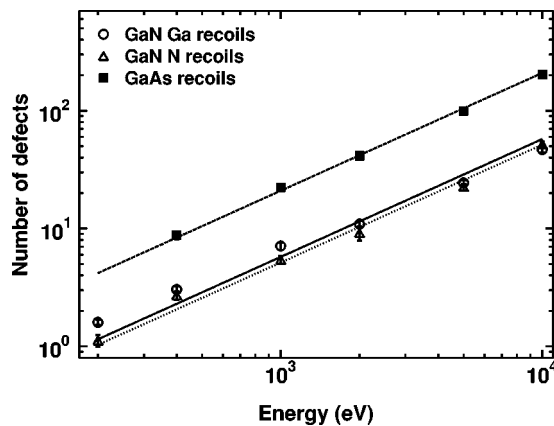


FIG. 2. Number of Voronoy defects produced by Ga and N recoils in GaN and linear fits to data. For comparison the damage production in GaAs is also shown. The GaAs data is from Ref. 24. Note that all the Ga recoil points at 200 eV–1 keV are clearly above the fitted line, indicating in-cascade recombination at higher energies.

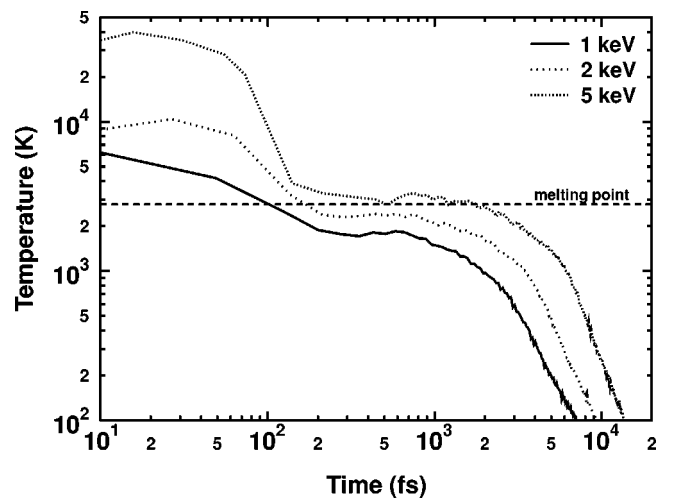


FIG. 3. Average temperature of area near cascade energy-weighted center.

TABLE II. Percentage of damage in clusters for N and Ga recoils in GaN.

E (keV)	Ga recoil	N recoil
1	20.7 ± 6.9	17.2 ± 6.2
2	21.8 ± 6.9	3.4 ± 3.4
5	30.8 ± 5.1	13.2 ± 4.7
10	23.1 ± 5.7	29.1 ± 6.7

mental differences.^{1,4,6} To examine the issue, we have simulated the amorphization process by successive 400-eV or 5-keV recoils.

The changes in volume and potential energy are shown in Fig. 4 as a function of irradiation dose. As in Si,¹⁵ the local heating caused by higher-energy recoils (1 keV versus 100 eV for Si and 5 keV versus 400 eV for GaN) relaxes defects with the highest potential energy and volume, and the resulting average potential energy and volume saturate to a smaller value. For both recoil energies the volume and the average potential energy saturate between 30 and 40 eV/atom dose. A large volume expansion (almost 20% with 400 eV) is observed during irradiation. Even larger expansions have been seen in experiments (about 50% in Ref. 5). This means that high internal stress is produced during irradiation.

The change in volume or potential energy is not a good measure of amorphous fraction due to the nonlinear relation to the number of defects. To get the amorphous fraction, we calculate the structure factor P_{st} (Ref. 19) for every atom i ,

$$P_{st} = \frac{1}{p_u(i)} \left(\sum_j [\theta_i(j) - \theta_i^p(j)]^2 \right)^{1/2}, \quad (1)$$

$$p_u(i) = \left(\sum_j [\theta_i^u(j) - \theta_i^p(j)]^2 \right)^{1/2}, \quad (2)$$

where $\theta_i(j)$ is a list of angles formed between the atom i and its neighbors, $\theta_i^p(j)$ is the distribution of angles in a perfect lattice, and $\theta_i^u(j) = j\pi/4(4-1)/2$ is the uniform angular dis-

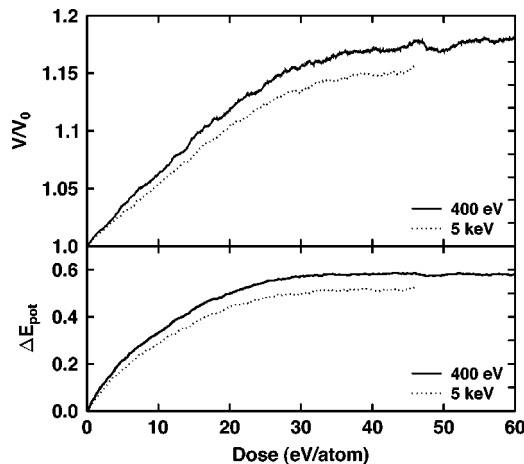


FIG. 4. Development of volume and potential energy compared to perfect crystal as a function of amorphization dose for GaN. Recoil energies of 400 eV and 5 keV were used.

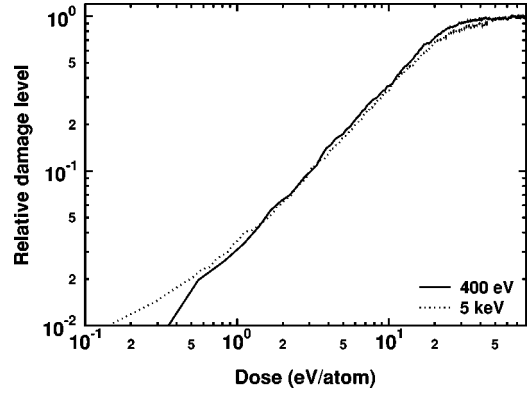


FIG. 5. Simulated amorphization fractions as a function of dose. Simulated values for 400-eV and 5-keV recoils are obtained by structure factor analysis.

tribution. Before taking the sum over angles the $\theta_i(j)$ lists are sorted by magnitude. All atoms for which P_{st} is larger than 0.125 are considered “defect” atoms. If a defect atom has at least three defect neighbors, it is defined as amorphous. A saturation value of the amorphous atoms in the 400-eV case was used as a reference point for full amorphization. The same method has previously been used in a study of amorphous fraction for Si, Ge, and GaAs.¹⁵

Figure 5 shows the simulated buildup of the amorphous fraction for 400-eV and 5-keV recoils. The amorphous fraction saturates below a dose of 40 eV/atom, which is lower than the experimental estimate of 90 eV/atom (Ref. 4) but much higher than that obtained for Si, Ge, and GaAs with the current method (about 10 eV/atom¹⁵). We therefore conclude that the high threshold displacement energy (leading to low damage production) and the in-cascade recombination can explain much of the high amorphization dose, but some recombination effect is not apparently reproduced by our method. This might be close Frenkel-pair recombination over long time scales at low doses or additional dynamic recoil-induced annealing¹¹ at the high doses.

It is noteworthy that the number of amorphous atoms for the 5-keV case saturates at a lower value than for the 400-eV case. This is consistent with the smaller volume expansion and the lower average potential energy in the 5-keV case. This may be due to the metal-like in-cascade recombination effect of molten areas or dynamic recoil-induced annealing of high-energy defects produced by earlier recoils. Since heavy ions produce more high-energy recoils, this difference may explain the variation in the saturation observed in experiments for different heavy ions.⁷

There are some other differences between the amorphous fraction buildups in the 400-eV and 5-keV cases. In the early stages of the process the amorphous fraction is higher for the 5-keV case, because the damage in 5-keV cascades is less scattered for the same dose than for the 400-eV case, and more atoms are counted as amorphous instead of isolated defects. With more irradiation, the roles change as the local heating in 5-keV cascades is able to recombine some of the damage, and the 5-keV case amorphizes about 20% slower than the 400-eV case. In the high-dose region the difference between the 400-eV and 5-keV cases grows even further, and

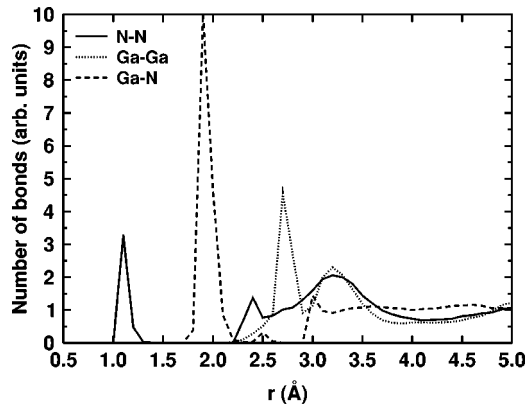


FIG. 6. Simulated partial pair-correlation functions of irradiated amorphous GaN. 400-eV recoils were used.

a 60% higher dose is needed for the 5-keV compared to the 400-eV case to reach an amorphization level of 85%. This indicates that the recombination by local heating (dynamic recoil-induced annealing¹¹) caused by high-energy recoils¹⁹ may be an important factor in the highly damaged region, and the use of higher than 5-keV recoils in the simulation can be estimated to lead to a higher amorphization dose.

D. Structure of amorphous material

To analyze the short-range order of the amorphized material, we calculated the full and partial pair-correlation functions of the irradiated GaN. The first peak in Fig. 6 at about 1.1 Å is a sign of segregated pure N gas formed by N-N dimers. The peak at about 2.0 Å is due to Ga-N bonds and the one at 2.7 Å is due to the weak Ga-Ga bonds in Ga-rich areas.

Bonding state analysis confirmed the formation of pure nitrogen gas. Cutoffs of 2.0 Å, 2.9 Å, and 2.9 Å were used for counting N-N, Ga-N, and Ga-Ga bonds, respectively. Figure 7 shows the formation of pure elements during irradiation. In this analysis, an atom is considered to be segregated if it has only like-atom bonds. The figure shows that pure nitrogen is produced at a constant rate during irradiation, but

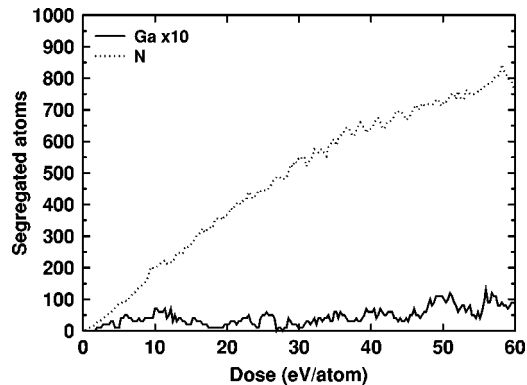


FIG. 7. Production of pure elements during irradiation. An atom is considered segregated if it has only like-atom bonds. The figure shows that pure nitrogen is produced at constant rate, but gallium-only regions are rare.

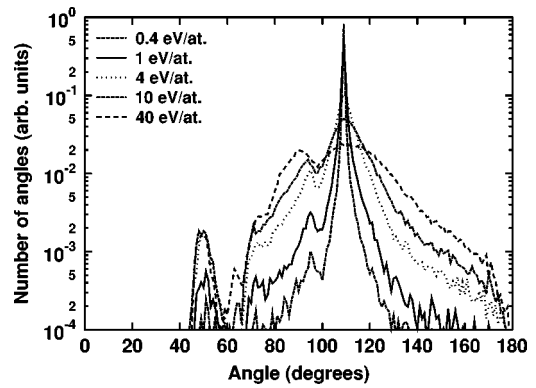


FIG. 8. Development of bond-angle distribution during irradiation.

although gallium-rich regions are produced, there is no sign of gallium-only regions at these doses.

Figure 8 shows the changes in the bond-angle distributions during the amorphization process. The main peak at 109° is widened and new peaks form at about 90° and 50°. The peak between 90° and 100° is formed by weak Ga-Ga bonds, which are generated after a small irradiation dose. After small distortions in the WZ lattice due to the initial damage, the gallium atoms form bonds with other gallium atoms in the WZ lattice. The gallium atoms move closer to each other, and the Ga-N-Ga angles are decreased.

Ring analysis methods were used to characterize the topological structure of the material. The prime rings, defined in Ref. 20 as rings with no shortcut, and the statistics of the shortest rings for bonds are shown in Table III. Only six-membered rings are found in the perfect crystal. In amorphized material five-membered and three-membered odd rings are dominant, with a significant amount of four-, six-, and seven-membered rings. It is interesting to note that a majority of the bonds belong to at least one ring with the size of 3. Only a few bonds have the shortest ring of size more than 7 and all bonds are members of at least one ring with size smaller than 11. The five-membered rings are more

TABLE III. Number of prime rings per atom and the shortest rings the atoms belong to in GaN amorphized by 400-eV recoils.

Ring size	Rings/atom	Shortest ring for bonds
3	0.576	0.62
4	0.347	0.22
5	0.581	0.13
6	0.463	0.021
7	0.310	0.0039
8	0.103	0.0017
9	0.067	0.0011
10	0.034	0.0004
11	0.035	0
12	0.023	0
13	0.018	0
14	0.010	0
15	0.007	0

common than the four-membered rings as the smallest ring size for bonds until the amorphization fraction reaches 0.5. The statistics shown in Table III remain stable during further irradiation.

IV. DISCUSSION

In our simulations of individual cascades, we found that much less damage is produced in GaN than in Si, Ge, or GaAs. Most of this (about a factor of 5) is explained by the higher threshold displacement energy of GaN. Another factor affecting the damage production in GaN is the enhanced in-cascade recombination effect akin to metals¹⁹ for high-energy (over 1 keV) recoils. The simulations also show that the damage in GaN cascades is very scattered, and most of the damage lies in point defects or small clusters. Since individual defects are easier to anneal than large clusters, a large amount of damage in GaN can be annealed after small irradiation doses (or recombined to more complex defects).

Many competing processes are involved in the amorphization of GaN,^{8,10} and different implantation conditions lead to very different amorphization dynamics. Point defect migration and recombination, dynamic and thermal annealing of clusters, chemical effects due to doping ions, preferential sputtering, local stoichiometric differences, ion specific primary cascade damage, and ion energy-dependent deposited energy density affect the outcome of ion beam implantations.^{5,7,8,10} Since some of these effects (long time scale and long-range processes) are not included in our model, the role of other effects can be observed more clearly. Our amorphization simulations describe high fluence low-temperature (less than 130 K, when defects are not mobile²¹) amorphization at the damage peak. Ion beam induced annealing of defects, local stoichiometric imbalance and segregation, and the structure and variation of individual cascade damage are well described in our model.

Amorphization proceeded in the simulations as follows. First highly separate damage and some clusters were produced by the initial recoils. This initial damage generated high stress and distortion in the lattice, where the second-nearest-neighbor Ga atoms started to form long “metallic” bonds with each other distorting the lattice even further. Gallium and nitrogen started to segregate, and nitrogen gas was produced throughout the process, in agreement with experimental observations.^{10,22,23} In the high damage region (amorphous fraction >50%) local heating started to recombine some of the damage produced by earlier recoils. This effect was larger for high-energy (5-keV) recoils than for low-energy (400 eV) recoils. Since heavier ions produce more high-energy recoils, this may explain the observed lower saturation damage level in the bulk damage peak for heavier ions during 300-K ion bombardment of GaN.⁷ At 40 eV/atom the amorphization was complete (although the fraction of atoms fulfilling our criterion for amorphous atoms was lower for the 5-keV than for the 400-eV recoils).

The amorphization dose in GaN, 40 eV/atom, is much higher than that obtained for Si, Ge, or GaAs with the same method,¹⁵ ~ 10 eV/atom. The main reason for the high amorphization dose in GaN is related to the high threshold

displacement energy leading to low damage production in individual cascades. Other factors are the in-cascade recombination in high-energy (>1 keV) cascades and the dynamic recoil-induced recombination of pre-existing damage in high-energy cascades leading to lower saturation damage level for the 5-keV recoils compared to the 400-eV recoils. Dynamic annealing effects, which have been proposed in earlier work^{1,4,6,11} are therefore confirmed by our simulations.

Although the amorphization dose we observe is much higher (a factor of ~ 5) than the dose in other semiconductors, it is still about a factor of 2 lower than the experimental value of 90 eV/atom (Ref. 4) at the border of the amorphous area in 180-keV Ar bombardment of GaN at 77 K temperature (we think that this value, which is determined at the amorphous frontier, is comparable to our simulations since the defects cannot escape the periodic cell to the outer crystalline lattice). Thus, since our simulations cannot fully reproduce the high amorphization dose of GaN, it is likely that in addition to the effects we do observe (high threshold energy and in-cascade and dynamic recoil-induced annealing), there are long time scale and long-range processes which our modeling cannot handle. Clearly further study is needed to fully understand the high variation of dose required for the amorphization of GaN during different implantation conditions.

V. CONCLUSIONS

We have studied the damage formation in bulk GaN during ion beam irradiation using molecular dynamics methods. Both individual cascades and amorphization during prolonged irradiation were studied.

Amorphization was found to start by formation of weak metallic Ga-Ga bonds in the distorted lattice. We observed nitrogen gas production during the irradiation, but not formation of pure gallium regions.

The simulations show that the high threshold displacement energy efficiently limits the damage in individual cascades. For high-energy recoils, in-cascade recombination similar to that in metals was observed. Also, during prolonged irradiation we observe dynamic recoil-induced annealing. Out of these three reasons, the first one leads to roughly a factor of 5 reduction in damage production compared to common semiconductors (Si, Ge, or GaAs), while the two others reduce the production less, a factor of 1–2 depending on conditions. These factors are shown to be the main reason for the high amorphization dose of GaN during low-temperature heavy-ion irradiation.

ACKNOWLEDGMENTS

The research was supported by the Academy of Finland under Project Nos. 48751, 50578, and 51585. Grants for computer time from the Center for Scientific Computing in Espoo, Finland are gratefully acknowledged.

- ¹H.H. Tan, J.S. Williams, J. Zou, D.J.H. Cockayne, S.J. Pearton, and R.A. Stall, *Appl. Phys. Lett.* **69**, 2364 (1996).
- ²C. Liu, B. Mensching, K. Volz, and B. Rauschenbach, *Appl. Phys. Lett.* **71**, 2313 (1997).
- ³C. Liu, B. Mensching, M. Zeitler, K. Volz, and B. Rauschenbach, *Phys. Rev. B* **57**, 2530 (1998).
- ⁴C. Liu, A. Wenzel, B. Rauschenbach, E. Alves, A.D. Sequira, N. Franco, M.F. da Silva, J.C. Soares, and X.J. Fan, *Nucl. Instrum. Methods Phys. Res. B* **178**, 200 (2001).
- ⁵S.O. Kucheyev, J.S. Williams, C. Jagadish, J. Zou, V.S.J. Craig, and G. Li, *Appl. Phys. Lett.* **77**, 1455 (2000).
- ⁶S.O. Kucheyev, J.S. Williams, C. Jagadish, J. Zou, and G. Li, *Phys. Rev. B* **62**, 7510 (2000).
- ⁷S.O. Kucheyev, J.S. Williams, C. Jagadish, J. Zou, and A.I. Titov, *Phys. Rev. B* **64**, 035202 (2001).
- ⁸W. Jiang, W.J. Weber, and S. Thevuthasan, *J. Mod. Opt.* **87**, 7671 (2000).
- ⁹E. Wendler, A. Kamarou, E. Alves, K. Gärtner, and W. Wesch, *Nucl. Instrum. Methods Phys. Res. B* **206**, 1028 (2003).
- ¹⁰S.O. Kucheyev, J.S. Williams, J. Zou, C. Jagadish, and G. Li, *Nucl. Instrum. Methods Phys. Res. B* **178**, 209 (2001).
- ¹¹We note that it is not always clear in the literature whether dynamic annealing is used to mean athermal annealing of preexisting defects by new recoils in the same spatial region, or thermally activated annealing occurring during the irradiation. In our work we use the phrase “dynamic recoil-induced annealing” to specify the former meaning.
- ¹²J. Nord, K. Albe, P. Erhart, and K. Nordlund, *J. Phys.: Condens. Matter* **15**, 5649 (2003).
- ¹³H.J.C. Berendsen, J.P.M. Postma, W.F. van Gunsteren, A. DiNola, and J.R. Haak, *J. Chem. Phys.* **81**, 3684 (1984).
- ¹⁴K. Nordlund, M. Ghaly, R.S. Averback, M. Caturla, T. Diaz de la Rubia, and J. Tarus, *Phys. Rev. B* **57**, 7556 (1998).
- ¹⁵J. Nord, K. Nordlund, and J. Keinonen, *Phys. Rev. B* **65**, 165329 (2002).
- ¹⁶J. Nord, K. Nordlund, and K. Albe (unpublished).
- ¹⁷A. Ionascut-Nedelcescu, C. Carlone, A. Houdayer, H.J. von Bardeleben, J.L. Cantin, and S. Raymond, *IEEE Trans. Nucl. Sci.* **49**, 2733 (2002).
- ¹⁸T. Diaz de la Rubia, R.S. Averback, R. Benedek, and W.E. King, *Phys. Rev. Lett.* **59**, 1930 (1987); **60**, 76(E) (1988).
- ¹⁹K. Nordlund and R.S. Averback, *Phys. Rev. B* **56**, 2421 (1997).
- ²⁰X. Yuan and A.N. Cormack, *Comput. Mater. Sci.* **24**, 343 (2002).
- ²¹K.H. Chow and G.D. Watkins, *Phys. Rev. Lett.* **85**, 2761 (2000).
- ²²S.O. Kucheyev, J.S. Williams, C. Jagadish, and S.J. Pearton, *Appl. Phys. Lett.* **76**, 3899 (2000).
- ²³S.O. Kucheyev, J.S. Williams, J. Zou, C. Jagadish, and G. Li, *Appl. Phys. Lett.* **77**, 3577 (2000).
- ²⁴K. Nordlund, J. Peltola, J. Nord, J. Keinonen, and R.S. Averback, *J. Appl. Phys.* **90**, 1710 (2001).